



**HAL**  
open science

## **Intracellular positioning systems limit the entropic eviction of secondary replicons toward the nucleoid edges in bacterial cells**

Charlene Planchenault, Marine Pons, Caroline Schiavon, Patricia Siguier, Jérôme Rech, Catherine Guynet, Julie Dauverd-Girault, Jean Cury, Eduardo Rocha, Ivan Junier, et al.

► **To cite this version:**

Charlene Planchenault, Marine Pons, Caroline Schiavon, Patricia Siguier, Jérôme Rech, et al.. Intracellular positioning systems limit the entropic eviction of secondary replicons toward the nucleoid edges in bacterial cells. 2019. hal-02366139

**HAL Id: hal-02366139**

**<https://hal.science/hal-02366139>**

Preprint submitted on 15 Nov 2019

**HAL** is a multi-disciplinary open access archive for the deposit and dissemination of scientific research documents, whether they are published or not. The documents may come from teaching and research institutions in France or abroad, or from public or private research centers.

L'archive ouverte pluridisciplinaire **HAL**, est destinée au dépôt et à la diffusion de documents scientifiques de niveau recherche, publiés ou non, émanant des établissements d'enseignement et de recherche français ou étrangers, des laboratoires publics ou privés.

Manuscript Number: JMB-D-19-00850

Title: Intracellular positioning systems limit the entropic eviction of secondary replicons toward the nucleoid edges in bacterial cells

Article Type: SI 2020: Chromosome folding

Section/Category: Sorting, spatiotemporal organization, trafficking, signal transduction and intracellular signaling

Keywords: plasmid; chromosome; partition; segregation; polymer unmixing

Corresponding Author: Dr. olivier espeli,

Corresponding Author's Institution: College de France

First Author: Charlene Planchenault

Order of Authors: Charlene Planchenault; Marine Pons; Caroline Schiavon; Patricia Siguiier; Jerome Rech; Catherine Guynet; Julie Dauverd-Girault; Jean Cury; Eduardo Rocha; Ivan Junier; Cornet Francois; olivier espeli

Abstract: Bacterial genomes, organized intracellularly as nucleoids, are composed of a main chromosome coexisting with different types of secondary replicons. Secondary replicons are major drivers of bacterial adaptation by gene exchange. They are highly diverse in type and size, ranging from less than 2 to more than 1000 kb, and must integrate with bacterial physiology, including to the nucleoid dynamics, to limit detrimental costs leading to their counter-selection. We show that large DNA circles, whether from a natural plasmid or excised from the chromosome tend to localize in a dynamic manner in a zone separating the nucleoid from the cytoplasm at the edge of the nucleoid. This localization is in good agreement with in silico simulations of DNA circles in the nucleoid volume. Subcellular positioning systems counteract this tendency, allowing replicons to enter the nucleoid space. In enterobacteria, these systems are found in replicons above 25 kb, defining the limit with small randomly segregated plasmids. Larger replicons carry at least one of the three described family of systems, ParAB, ParRM and StbA. Replicons above 180 kb all carry a ParAB system, suggesting this system is specifically required in the cases of large replicons. Simulations demonstrated that replicon size profoundly affects localization, compaction and dynamics of DNA circles in the nucleoid volume. The present work suggests that presence of partition systems on the larger plasmids or chromids is not only due to selection for accurate segregation but also to counteract their unmixing with the chromosome and consequent exclusion from the nucleoid.

Suggested Reviewers: Christine Jacobs wagner  
Yale University  
christine.jacobs-wagner@yale.edu

Rodrigo Reyes-Lamothe  
McGill University, Montreal, Canada

rodrigo.reyes@mcgill.ca

Martin Thanbichler  
Phillips University, Marburg  
thanbichler@uni-marburg.de

Marco Consentino Lagomarsino  
IFOM, FIRC Institute of Molecular Oncology, Milan, Italy  
marco.cosentino-lagomarsino@upmc.fr

Paul Wiggins  
Department of Physics, University of Washington, USA  
pwiggins@uw.edu

Joe Pogliano  
Division of Biological Sciences, University of California, San Diego, San  
Diego, CA 92093  
jpogliano@ucsd.edu

Opposed Reviewers: Suckjoon Jun  
UCSD  
jun@ucsd.edu

COLLÈGE  
DE FRANCE  
—1530—

Centre Interdisciplinaire de Recherche en Biologie - UMR CNRS 7241 / INSERM U1050

Equipe "Dynamique des Chromosomes"

Paris, le 31 juillet 2019

**Olivier ESPELI**

T. +33 (0)1 44 27 12 49

[olivier.espeli@college-de-france.fr](mailto:olivier.espeli@college-de-france.fr)

Dear Romain Koszul and Marcelo Nollmann,

Please find enclosed a manuscript entitled "**Intracellular positioning systems limit the entropic eviction of secondary replicons toward the nucleoid edges in bacterial cells.**" that we are submitting for publication for the special issue of Journal in Molecular Biology *Perspectives on chromosome folding*.

Our analysis combined genomic dissection, genetic engineering, fluorescence microscopy methods and in silico models to characterize the localization and dynamics of bacterial secondary replicons. Bacterial genomes, organized intracellularly as nucleoids, are composed of a main chromosome coexisting with different types of secondary replicons. Secondary replicons are major drivers of bacterial adaptation by gene exchange, including the acquisition of virulence and resistance to antibacterial compounds. They are highly diverse in type and size, ranging from less than 2 to more than 1000 kb, and must integrate with bacterial physiology, including to the nucleoid dynamics, to limit detrimental costs leading to their counter-selection. We show that large DNA circles, whether from a natural plasmid or excised from the chromosome tend to localize in a dynamic manner in a zone separating the nucleoid from the cytoplasm at the edge of the nucleoid. We demonstrate that presence of partition systems on the larger plasmids or chromids is not only due to selection for accurate segregation but also to counteract their unmixing with the chromosome and consequent exclusion from the nucleoid.

We discuss these observations in the context of the biophysics of cell organization and the evolution of bacterial genomes.

I enclose the names and addresses of four potential referees: Dr. Paul Wiggins, Dr Rodrigo Reyes Lamothe, Pr. Christine Jacobs Wagner, Dr. Martin Thanbichler

Thank you very much,  
Sincerely yours

Olivier Espéli  
Directeur de Recherche CNRS



Equipe "Dynamique des Chromosomes"

Paris, le 31 juillet 2019

**Olivier ESPELI**

T. +33 (0)1 44 27 12 49

[olivier.espeli@college-de-france.fr](mailto:olivier.espeli@college-de-france.fr)**Potential referees****Intracellular positioning systems limit the entropic eviction of secondary replicons toward the nucleoid edges in bacterial cells****Dr. Paul Wiggins**

Department of Physics, University of Washington, USA

[pwiggins@uw.edu](mailto:pwiggins@uw.edu)**Pr Christine Jacobs Wagner**

Microbial Sciences Institute

WC-ABC 2nd floor, room 269

Yale University

USA

[christine.jacobs-wagner@yale.edu](mailto:christine.jacobs-wagner@yale.edu)**Dr Rodrigo Reyes Lamothe**

Department of Biology, McGill University

Montreal, Quebec H3G 0B1, Canada

[rodrigo.reyes@mcgill.ca](mailto:rodrigo.reyes@mcgill.ca)**Pr. Martin Thanbichler**

Faculty of Biology

c/o Faculty of Chemistry (room C233)

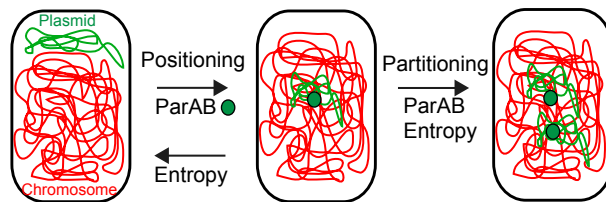
Philipps University

Hans-Meerwein-Str. 4

35043 Marburg

Germany

[thanbichler@uni-marburg.de](mailto:thanbichler@uni-marburg.de)



## \*Research Highlights

- \* Secondary replicons above 25 kb always encode at least one partition system
- \*The ParAB partition system serves as a positioning system to maintain large replicons within the nucleoid
- \*DNA plasmids lacking a partitioning system are localized to the edge of the nucleoid
- \* Positioning at the nucleoid edge is akin to polymer unmixing observed in simulations

# Intracellular positioning systems limit the entropic eviction of secondary replicons toward the nucleoid edges in bacterial cells

Charlene Planchenault<sup>1</sup>, Marine Pons<sup>2</sup>, Caroline Schiavon<sup>2</sup>, Patricia Siguier<sup>2</sup>, Jérôme Rech<sup>2</sup>, Catherine Guynet<sup>2</sup>, Julie Dauverd – Girault<sup>1</sup>, Jean Cury<sup>3</sup>, Eduardo PC Rocha<sup>3</sup>, Ivan Junier<sup>4</sup>, François Cornet<sup>2</sup>, Olivier Espéli<sup>1\*</sup>

<sup>1</sup> Center for Interdisciplinary Research in Biology – Collège de France, CNRS UMR7241, INSERM U1050, PSL University

<sup>2</sup> Laboratoire de Microbiologie et Génétique Moléculaires (LMGM), Centre de Biologie Intégrative (CBI), Centre National de la Recherche Scientifique (CNRS), Université Paul Sabatier – Toulouse 3, 31000, Toulouse, France.

<sup>3</sup> Microbial Evolutionary Genomics, Institut Pasteur, CNRS, UMR3525, Paris, France

<sup>4</sup> TIMC-IMAG, CNRS UMR5525 - Université Grenoble Alpes, Campus Santé - Institut Jean Roget

\* to whom correspondence should be sent: [olivier.espeli@college-de-france.fr](mailto:olivier.espeli@college-de-france.fr)

## Abstract

Bacterial genomes, organized intracellularly as nucleoids, are composed of a main chromosome coexisting with different types of secondary replicons. Secondary replicons are major drivers of bacterial adaptation by gene exchange. They are highly diverse in type and size, ranging from less than 2 to more than 1000 kb, and must integrate with bacterial physiology, including to the nucleoid dynamics, to limit detrimental costs leading to their counter-selection. We show that large DNA circles, whether from a natural plasmid or excised from the chromosome tend to localize in a dynamic manner in a zone separating the nucleoid from the cytoplasm at the edge of the nucleoid. This localization is in good agreement with *in silico* simulations of DNA circles in the nucleoid volume. Subcellular positioning systems counteract this tendency, allowing replicons to enter the nucleoid space. In enterobacteria, these systems are found in replicons above 25 kb, defining the limit with small randomly segregated plasmids. Larger replicons carry at least one of the three described family of systems, ParAB, ParRM and StbA. Replicons above 180 kb all carry a ParAB system, suggesting this system is specifically required in the cases of large replicons. Simulations demonstrated that replicon size profoundly affects localization, compaction and dynamics of DNA circles in the nucleoid volume. The present work suggests that presence of partition systems on the larger plasmids or chromids is not only due to selection for accurate segregation but also to counteract their unmixing with the chromosome and consequent exclusion from the nucleoid.

## Introduction

Bacterial genomes are compact and highly organized both at the genetic and physical levels. Genome organization results from the need of a compromise between folding chromosomes much longer than bacterial cells and favoring the interaction between DNA and machineries implicated in processes such as transcription, replication and segregation. Bacterial genomes are composed of one main chromosome and most often contain secondary replicons. Main chromosomes range from few hundred to over ten thousand kilobases (kb) and are the largest replicon in the cell. Secondary replicons comprise a plethora of plasmids, highly variable in size, along with larger replicons (> 500 kb) called secondary chromosomes or chromids that are found in genomes across a species (Smillie *et al*, 2010) . It is generally admitted that secondary replicons fall in three categories: small multicopy plasmids, large low copy-number plasmids and chromids. Plasmids carry numerous adaptive functions, including numerous virulence factors, and are the major drivers of the transfer of antibiotic resistance genes. Most plasmids are relatively small (less than 150 kb) but may together account for up to 30% of the genome. Chromids (Harrison *et al*, 2010), secondary chromosome above 500kb, are frequent and appeared independently in several taxa. They originate from plasmids – from different plasmid families depending on species - as judged by the sequence of their replication origins (e.g. Ramachandran *et al*, 2017). How and why some plasmids are domesticated as chromids is currently poorly understood. Large plasmids and chromids often carry complex traits involved in bacteria-eucaryote interaction in infections and symbiosis processes (e.g. Marchetti *et al*, 2010)

Depending on the plasmid and its interaction with its genetic background, plasmids can be costly because of the metabolic burden imposed by plasmid replication, the consumption of resources for the expression of plasmid-encoded genes, synthesis of the plasmid conjugation apparatus, alteration in the expression of host genes or fine-tuning cellular pathways, and other metabolic effects such as the introduction of efflux pumps transporting important biomolecules (Baltrus, 2013). Previous studies have also demonstrated that although plasmids initially impose fitness cost to host strains, the cost could be compensated after passage of hundreds of generations (Carroll & Wong, 2018; Bouma & Lenski, 1988) Acquisition of plasmid stabilization system such as poison-antidote systems (toxin/ antitoxin or restriction-modification) and resolution system can enhance the persistence of plasmids.

Small multicopy plasmids are thought to both replicate and segregate following a "random copy choice" model. However, many natural (non-engineered) bacterial plasmids are low copy. The low copy number plasmids necessitate active partition to avoid loss from random segregation during cell doubling (Reyes-Lamothe *et al*, 2014). Specific molecular mechanisms - partition systems - limit the impact of plasmid cost on their maintenance by reducing the rate of plasmid loss by thousands fold (Bouet & Funnell, 2019). Plasmid segregation follows DNA replication and involves the separation and transportation of the two copies of the replicon in opposite directions along the longitudinal cell axis (Gordon *et al*, 1997; Sengupta *et al*, 2010), which ensures that every daughter cell receives at least one copy of the plasmid. Almost all partition systems identified to date consist of three components, one or more copies of a partition site (the "centromere"), a centromere-binding protein, named ParB or ParR and an NTPase (ATPase or GTPase) named ParA or ParM. Studies reporting the intracellular localization of specific DNA loci in bacterial cells revealed that F, P1 and RK2 plasmids are preferentially found around mid- or quarter-cell positions colocalized with the bacterial nucleoid and confirmed that the partition process is a positioning process within the cell .

1 However, plasmids belonging to different incompatibility groups are tethered to different sites within  
2 the cell, and segregate at different times relative to one another and to the bacterial cell cycle (Ho *et*  
3 *al*, 2002). Small plasmids lacking partition systems such as ColE1-type plasmids also form clusters but  
4 at the nucleoid periphery (Reyes-Lamothe *et al*, 2014). In addition, evidence indicates that the  
5 bacterial chromosome compacted in the nucleoid contributes both passively (as the major structure  
6 occupying space inside a bacterial cell) and actively (as a support and/or matrix for plasmid  
7 movement) to plasmid partition mechanisms (Le Gall *et al*, 2016; Derman *et al*, 2008). F and P1  
8 plasmids without Par systems are excluded from the nucleoid (Niki & Hiraga, 1997; Erdmann *et al*,  
9 1999; Le Gall *et al*, 2016), but Par + plasmids are not. The reason why plasmids deleted for their  
10 partition system are excluded from the nucleoid is not understood.  
11  
12

13  
14 In the present work we analysed the completely sequenced genomes of enterobacteria to survey the  
15 presence of partition systems encoded by secondary replicons. We observed that partition systems  
16 are present in replicons with a characteristic size above 25kb, and lacking in smaller plasmids. We  
17 postulated therefore that the size of a plasmid is a critical determinant of its cost independently of  
18 the genes that it encodes. To experimentally test this hypothesis, we analysed the localization, the  
19 dynamics and the loss frequency of the large R27 plasmid from which we perturbed the partition  
20 systems. As observed for other plasmids localization of the R27 plasmid in the nucleoid depends on a  
21 functional ParABS system, we therefore wanted to test if such nucleoid exclusion is not the default  
22 localization of circular DNA elements in *E. coli*. To test this hypothesis we monitored the localization  
23 of a large DNA circle excised from the chromosome and performed in silico simulation of polymer  
24 circles localization within nucleoid. .  
25  
26  
27  
28  
29

30 Our results indicate that the R27 plasmid lacking partition are more frequently localized at the pole  
31 of the cell at the edge of the nucleoid. We observed a similar localization and mobility characteristics  
32 for large DNA circles excised from the chromosome. Simulations suggest that this polar exclusion can  
33 be explained by the sole force of entropic repulsion of the polymers. We observed that circles and  
34 plasmid do not occupy DNA free regions but rather localized at the transition between the cytoplasm  
35 and the nucleoid, suggesting that large DNA molecules do not get access easily to the cytoplasm of *E.*  
36 *coli*. Localization at the nucleoid – cytoplasm frontiers can be disadvantageous for various DNA  
37 metabolic processes such as replication, transcription or recombination that happen in the nucleoid  
38 core. This leads us to propose that, in addition to assist the correct segregation of replicated  
39 plasmids, partition systems have the function of targeting plasmids to the nucleoid. We further  
40 propose that this is advantageous for them.  
41  
42  
43  
44  
45  
46  
47

## 48 **Results**

### 49 **The size of the plasmid determines the presence and the type of partition systems**

50  
51 To study the distribution of subcellular positioning systems in secondary replicons, we selected 971  
52 secondary replicons from sequenced Enterobacterial genomes. These were representative of the  
53 different replicon families as judged by the diversity of their replication origins and initiator proteins  
54 (Rep types) as well as their transfer functions (MOB types). They ranged from 1.3 to 794 kb in size  
55 and show a clear bimodal size distribution with a separation between peaks at around 25 kb (Figure  
56 1). 25% were less than 25 kb. The repartition of sizes was then monotonous from 30 to 120 kb except  
57  
58  
59  
60  
61  
62  
63  
64  
65

1 for a large over-representation of 90 to 100 kb plasmids (11% of total); 23% were longer than 130 kb  
2 but only 1% were longer than 200 kb and 7 were chromids (> 500 kb). Very large secondary replicons  
3 are thus rare in Enterobacteria. We searched for three types of subcellular positioning / segregation  
4 systems: ParAB, ParRM and StbA (Figure 1). The well-described ParAB and ParRM systems were  
5 searched using appropriate HMM profiles (SupTable 1,(Cury *et al*, 2017)). The StbA protein,  
6 experimentally studied in R388, was searched by similarity using the six *stbA* alleles previously  
7 identified (Gynet *et al*, 2011). Figure 1 shows the presence of these three systems in plasmids  
8 ranked by the size of the latter. The vast majority of small plasmids lack any system. In contrast, most  
9 larger plasmids and chromids possess at least one system. The transition between these two types of  
10 replicons occurs around 25 kb, consistent with the minimum of plasmid size distribution. Only 5  
11 plasmids shorter than 25 kb had a potential positioning system. The ParAB system was more  
12 frequent than the ParRM and StbA systems. Strikingly, all plasmids above 180 kb, including the  
13 chromids, had a ParAB homolog. StbA was mostly present in medium-sized plasmids (34-148 kb).  
14 ParRM systems were more evenly distributed than StbA. However, their occurrences in replicons  
15 above 180 kb were always accompanied by the presence of a ParAB system.

16  
17  
18  
19  
20  
21 The more detailed analysis of the 79 plasmids longer than 25 kb and lacking partition systems  
22 revealed potential ParAB or ParMR systems that did not score well enough in the automatic  
23 annotation or contained frameshifts. Some of the latter may result from sequencing errors (60  
24 plasmids, Sup Table 2). We found that many of the remaining large plasmids lacking partition systems  
25 contained ribosomal operons, were almost entirely composed of bacteriophages or mobile genetic  
26 elements. We concluded that: (i) partition systems are effectively essential for plasmids above 25kb  
27 long in Enterobacteria; (ii) a ParAB system is specifically required for plasmids above 180 kb, and this  
28 includes all the chromids.

### 32 33 34 35 **Localisation and dynamics of the R27 megaplasmid strongly depends on ParAB but not on ParRM**

36  
37 The above data suggest that large plasmids specifically require a ParAB system for their maintenance.  
38 To study the role of ParAB in a large plasmid, we use R27, a 180 kb long natural IncHI2 plasmid  
39 carrying resistance to tetracycline (Taylor, 1983) . As all IncHI2 plasmids, R27 codes for both a ParAB  
40 and a ParRM system. Both systems were reported to be able to stabilize an unstable cloning vector  
41 and involved in R27 maintenance and subcellular positioning, although the ParAB system had a larger  
42 effect (Lawley and Taylor, 2003). We first analysed the R27 sequence and detected a toxin-antitoxin  
43 (TA) system not previously annotated, which may impair stability assays. This TA system was deleted  
44 and replaced by the *lacI* gene, allowing a coloured detection of plasmid less colonies on agar plates in  
45 an otherwise  $\Delta(lacI)$  strain. Using this system, we confirmed the previous findings on the role of the  
46 ParAB and ParRM systems on R27 maintenance (SupFig 1). R27 $\Delta$ (TA) was stable over 60 generation  
47 of growth. Its  $\Delta(parAB)$  derivative was lost whatever the growth conditions (L-broth or M9 broth  
48 supplemented with glycerol and casamino acids), although loss was more frequent during rapid  
49 growth (L-broth). This contrasted with the  $\Delta(parRM)$  derivative, which was lost only during rapid  
50 growth. This confirms that ParAB is the prominent system for R27 stability.

51  
52  
53  
54  
55  
56  
57 When tagged with a FROS system, R27 derivatives were shown to localise plasmids (Lawley and  
58 Taylor, 2003). Single foci tended to localise close to mid-cell, whereas two or more foci localised  
59 symmetrically along cell length. These localisations depended on the ParAB system and to a lesser  
60

1 extent on the ParRM system. To further explore the role of the two Par systems, we tagged our R27  
2 derivatives with a *parS<sub>P1</sub>* site and transfer them into strains producing a GFP-ParB fusion protein from  
3 a  $\Delta(lacZ)::gfp-parB_{P1}$  chromosomal construct (Stouf *et al*, 2013). R27 $\Delta$ (TA) localized in the midcell  
4 zone when present as a single focus and towards the cell quarters in cells with two foci. The  
5  $\Delta(parAB)$  derivative do not present this localisation whereas no defect was detectable for the  
6  $\Delta(parRM)$  derivative (Figure 1B - D). We thus confirm that R27 localises as the smaller plasmids F, P1  
7 and R388 plasmids, showing its large size does not preclude localisation inside the nucleoid and that  
8 this effect depends on ParAB.  
9

10  
11 Taken together, our data suggest that large plasmids strictly need a ParAB system for their  
12 maintenance. ParAB maintain plasmid copies inside the nucleoid whatever their size, whereas ParRM  
13 systems don't. When devoid of ParAB systems, large plasmids exit the nucleoid and localize in a  
14 dynamic manner at the polar nucleoid edge. Localising inside the nucleoid may thus be especially  
15 important for very large plasmids and chromids. To understand why this should be, we performed  
16 simulations of secondary replicon dynamics of different sizes.  
17  
18  
19  
20  
21  
22

### 23 **Polymer modeling shows that plasmids are evicted from the nucleoid**

24  
25 In silico simulations of DNA and chromosome polymers have been extremely useful to evaluate  
26 physics of chromosome and plasmid conformation and segregation (Vologodskii & Cozzarelli, 1993;  
27 Vologodskii *et al*, 1992; Jun & Mulder, 2006; Junier *et al*, 2014). Monte Carlo simulations revealed  
28 that bacterial chromosomes unmix in the confined environment formed by the nucleoid shell (Jun &  
29 Mulder, 2006). We used simulations to evaluate if the localization and conformation of plasmids  
30 lacking partition systems was a consequence of entropy-mediated unmixing of polymers. We  
31 simulated a 3D nucleoid containing one chromosome and one plasmid over tens of millions of  
32 iterations (simulation steps). The nucleoid volume was defined by a cylinder with a long axis of 2000  
33 nm and a diameter of 800 nm (Figure 2A). The chromosome was modeled using a 40 nm thick semi-  
34 flexible chain accounting for the nucleoprotein structure that has been observed in rapidly dividing  
35 cells with a 100bp/nm base-pair density and a persistence length of 100 nm that is much smaller  
36 than the diameter of the nucleoid. In practice, the simulations were performed by discretizing the  
37 chromosome and plasmid chains using 30 nm long cylinders (1392 cylinders in total for the  
38 chromosome). Plasmid size was varied from 30 kb (9 cylinders) to 1400 kb (423 cylinders). Finally, to  
39 quantify the impact of chromosome on the location properties of plasmids we used, as a control,  
40 simulations where only the plasmid was present in the nucleoid shell. Localizations of plasmids in the  
41 absence of a chromosome dramatically differed from that of plasmids evolving in a chromosome  
42 crowded nucleoid cell (Supplementary Figure S2 and S3).  
43  
44  
45  
46  
47  
48  
49

50  
51 We first quantified the localization of plasmids along the long axis of the nucleoid as a function of  
52 their size ( $L_p$ ). Plasmids with less than 100 kb, localized at approximately similar frequencies inside  
53 and outside of the area defined by the chromosome edges, whereas large plasmids resided  
54 preferentially on the outside of the chromosome (Figure 2B and Figure 3A). Along the short axis of  
55 the nucleoid, the barycenter of small plasmids was found with equal probability on the edge or near  
56 the center of the nucleoid volume while the barycenter of large plasmid was mainly observed closer  
57 to nucleoid center (Figure 3A). This behavior was significantly different than what we observed for  
58 plasmid evolving in an empty nucleoid shell (Supplementary Figure S1). The results of these  
59  
60  
61  
62  
63  
64  
65



1 simulations are in good agreement with the polar localization observed for F (Le Gall *et al*, 2016) or  
2 R27 plasmids lacking a partition system (Figure 1B - D). This suggests that partition systems may  
3 counteract entropy mediated unmixing of plasmid and chromosomes and to allow plasmids to enter  
4 in the main nucleoid volume. Even if the unixed state is frequent, we observed plasmids localized in  
5 between chromosome edges when they were traveling from one side to the other of the nucleoid  
6 (Figure 2B). Observation of few examples suggested that plasmid traveling across the nucleoid pass  
7 on the side of the chromosome (Figure 3B). To check how frequently plasmid and chromosome  
8 actually overlap, we measured the distance of the plasmid barycenter from the nucleoid center on  
9 the short cell axis as a function of their position along the long nucleoid axis (Figure 3C). We observed  
10 the same trend for small (100kb) and large (600kb) plasmids: when they localized over the  
11 chromosome on the long axis of the nucleoid, they were excluded from the nucleoid center on the  
12 short axes (Figure 3C). Interestingly, small plasmids were also pushed toward lateral edges of the  
13 nucleoid when at the pole, while large plasmids were not. This positioning was dramatically different  
14 in a chromosome free shell (Supplementary Figure S2). We conclude that plasmids and  
15 chromosomes are mostly unmixed whatever their size and position in the nucleoid.  
16  
17  
18  
19  
20  
21  
22

### 23 **The length of the plasmid determines its compaction within nucleoid**

24  
25 The simulations allowed us to question several aspects of the interplay between plasmids and the  
26 chromosome. First, we tested if plasmid and chromosome compaction was modulated by plasmid  
27 size. We used plasmid and chromosome spreading, i.e. the longitudinal or lateral extension of  
28 plasmids and chromosome as a proxy of their compaction within nucleoid. Our simulations were  
29 performed with a fixed nucleoid volume. First, plasmid spreading was measured along the short or  
30 the long axis of the nucleoid. Plasmid spreading was directly dependent on the size of the plasmid  
31 and the presence chromosomal DNA (Figure 4A and Supplementary Figure S2). Plasmid spreading  
32 decreased following a power law with plasmid size. Longitudinal chromosome spreading was only  
33 modestly affected by the presence of plasmid. Large plasmids (>1000 kb), however, imposed a  
34 reduction of the chromosome extension by 15% (Figure 4A). Interestingly, in the presence of the  
35 chromosome, plasmid compaction (the longitudinal spread of plasmid normalized by its size, NLS)  
36 was dramatically dependent on plasmid size. NLS follows a power law,  $NLS = A * L_p * e^{-0.5}$  (Figure 4B).  
37 Plasmids above 700 kb were compacted to the level of the chromosome while smaller plasmids were  
38 much less compacted (Figure 4B). For plasmids below 100 kb the compaction was not significantly  
39 changed by the presence of chromosome compared to the empty nucleoid shell (Figure 4B). These  
40 results suggest that if the nucleoid volume is maintained constant in the cell, plasmid larger than 100  
41 kb will be compacted to fit in the nucleoid volume; this compaction will be severe for the largest  
42 plasmids.  
43  
44  
45  
46  
47  
48  
49  
50  
51  
52

### 53 **Mobility of plasmid polymers**

54  
55 We observed plasmid trajectories crossing the nucleoid. Because Monte-Carlo simulations are  
56 dedicated (in principle) to quickly reach equilibrium, they may not be suitable for dynamical analyses.  
57 However, accepted motions in our model correspond to small, local deformations of the chain, and  
58 thus often provide a good estimation of the resulting large-scale dynamics of systems. Simulation  
59  
60  
61  
62  
63  
64  
65

1 traces show that plasmid localizations were highly similar between short interval iterations,  
2 suggesting that localization at iteration N was not completely independent from the localization at  
3 iteration N-1. As a consequence, we can analyze plasmid trajectories. In this context, we first  
4 measured how frequently plasmids cross the chromosome territory along the long axis of the cell  
5 (Figure 4C). This parameter might be important when considering random segregation of plasmids  
6 without partition machinery. We observed that crossing frequency exponentially decayed with  
7 plasmid size. In the length of our simulations ( $>5e10^7$  steps) plasmids above 1MB extremely rarely  
8 crossed the chromosome territory. When plasmids were smaller than 600 kb, both the frequency  
9 (Figure 4C) and the speed (Figure 4D) of crossing events were strongly dependent on their size. We  
10 measured the average velocity of nucleoid crossings in the 200 kb plasmid simulation and compared  
11 it to the reptation of an individual chromosomal locus (Figure 4E). Plasmid crossings were much  
12 faster than reptations of chromosomal loci. This suggests that unmixing of polymers is much more  
13 efficient than reptation inside a single polymer. Rapid unmixing has been already observed for 2  
14 chromosome polymers of equal size (Jun & Mulder, 2006) but, to our knowledge, this was not  
15 described for two polymers of different sizes in a nucleoid like confinement. Finally, we measured  
16 mobility of plasmids at their polar position; it showed that mobility of small plasmids was higher than  
17 that of large plasmids and chromosome (Figure 4F). The velocity of plasmids that crossed the  
18 nucleoid (Figure 4E) was comparable (9 nm / 1000 iterations for a 200 kb plasmid) to that of plasmid  
19 at their polar home position (8.2 nm /1000 iterations for a 200 kb plasmid). Therefore during  
20 nucleoid crossing the directionality is imposed by a higher frequency of correlated movements but  
21 not by an acceleration (Figure 4E).  
22  
23  
24  
25  
26  
27  
28  
29  
30

### 31 **Localization and dynamics of DNA circles and R27plasmids**

32  
33  
34 In the purpose to confirm R27 experiments and simulations with a heterologous system, we used an  
35 assay designed by F. Boccard and colleagues that allows excision of large DNA segments from the  
36 chromosome as DNA circles. The excised segment is tagged with a parS/parBGFP system to image its  
37 localization and dynamics. The strain also expresses a HupA-mCherry fusion to visualize the nucleoid.  
38 We have chosen to excise a 137 kb segment of the chromosome 400kb away from oriC. Before  
39 excision, this locus presented the typical patterns of localization of the oriC region, cells with 2 to 4  
40 foci localized at the quarters and 1/8 of the cell. Following induction of the recombinase for 30 min (a  
41 sufficient induction to nearly reach 100% of excision) the localization of the ParB-GFP foci  
42 dramatically changed, most cells presented one focus localized at the edge or at the middle of the  
43 nucleoid (Figure 5A). This polar localization is akin to the localization observed with the R27 plasmid  
44 lacking the partition system. The frequency of polar foci was higher for the excised circles (75%)  
45 compared to the R27 plasmid lacking parAB system (35%), suggesting that R27  $\Delta$ parAB keeps some  
46 nucleoid targeting elements, may be the ParRM system. These results demonstrate that DNA circles  
47 lacking positioning system tend to be positioned at the nucleoid edge.  
48  
49  
50  
51  
52  
53

54 We used time lapse microscopy to evaluate the mobility of the excised circle and R27 plasmid (Figure  
55 5B). Kymographs of plasmid lacking ParAB and excised foci differed significantly from that of  
56 chromosomal foci (Figure 5B). At long time scale we observed, with the excised circles and the  
57 R27 $\Delta$ parAB plasmid, frequent long, rapid and oriented movements. These movements frequently  
58 produced merging of foci (Figure 5B). These movements consisted in foci moving from the nucleoid  
59  
60  
61  
62  
63  
64  
65

1 toward the cell pole or toward the nucleoid free mid-cell zone (Figure 5C). Chromosomal loci also  
2 presented ballistic like movements but they mainly corresponded to segregation events and they  
3 were confined to the nucleoid area. We measured that average velocity of ballistic movements of  
4 excised circles and chromosomal loci segregating. Velocity of nucleoid crossing by excised circles  
5 toward cell pole is  $142 \pm 80 \text{ nm}\cdot\text{min}^{-1}$  (N=50), this is 3 times faster than the average velocity of  
6 chromosomal loci segregating from quarter positions,  $50 \pm 30 \text{ nm}\cdot\text{min}^{-1}$  (N=50). Using the same  
7 localization system, P. Wiggins and colleagues observed that most chromosomal loci present a  
8 maximal drift velocity,  $\approx 300 \text{ nm}\cdot\text{min}^{-1}$ , immediately after foci splitting (Cass *et al*, 2016). Two  
9 minutes later drift velocity has already slowed down to  $20 - 50 \text{ nm}\cdot\text{min}^{-1}$  to finish segregation in 20  
10 min. Here we observed prolonged high velocity movements of excised circles, they might correspond  
11 to the ballistic movements observed in the simulation; therefore they can give an estimation of the  
12 efficiency of entropy mediated unmixing in these experimental conditions. At shorter time scale  
13 ballistic movements were not observed (Figure 5B). Excised circles resided stably at the nucleoid  
14 edges, R27 plasmid lacking the ParAB system were also stable on the long axis of the cell. By contrast  
15 we still observed significant longitudinal movement of the R27 and chromosomal locus. We  
16 measured Mean Squared Displacement (MSD) to obtain quantitative analysis of the mobility of foci  
17 (Figure 5D - G). MSD curves were characteristic of subdiffusive motions, following a power law:  $\text{MSD}$   
18  $= D \cdot \Delta T^\alpha$  where D is coefficient of diffusion,  $\Delta T$  the time interval and  $\alpha$  the scaling exponent. MSD  
19 confirmed that excised foci present a different mobility compared to chromosomal loci (Figure 5D  
20 and 5E). For time intervals around 2 sec, their MSD  $\alpha$  coefficient is reduced (0.43 vs 0.48), their  
21 coefficient of diffusion is reduced ( $0.0044$  vs  $0.0053 \text{ }\mu\text{m}^2 \cdot \text{sec}^{-1}$ ), the cage surrounding their  
22 movements is also reduced by a factor of 2 and the average distance that they travel in one interval  
23 is 20 % reduced. Mobility of WT R27 plasmid differed from that chromosomal loci or excised circles  
24 ( $\alpha = 0.66$  and  $D = 0.0026 \text{ }\mu\text{m}^2 \cdot \text{sec}^{-1}$ , Figure 5F and 5G). The absence of the ParAB system dramatically  
25 reduces the mobility of R27. It was particularly striking for the coefficient of diffusion that dropped to  
26  $0.001 \text{ }\mu\text{m}^2 \cdot \text{sec}^{-1}$ . Our observations demonstrate, for every dynamics parameters, that R27 plasmid  
27 lacking ParAB behavior is akin but not strictly identical to the excised circle.

### 40 **Nucleoid edges serves as a platform for DNA circle surfing**

41  
42 Differently from the simulations we observed that plasmids lacking partition systems and excised  
43 circles were less mobile than chromosomal loci. This suggests that the nucleoid edge is not a  
44 constrain-free localization. To understand what is constraining the mobility of excised circles and  
45 plasmids at the nucleoid edges, we investigated this localization in more details. Fluorescence  
46 quantification suggested that circle foci localized precisely at the edges of the nucleoid but do not  
47 freely navigate in the DNA free zone at the pole of cell (Figure 6A). As illustrated for one example, we  
48 observed frequently that mobility along the short axis of the cell is higher for excised loci compared  
49 to mobility along the long axis of the cell (Figure 6B). We deconvoluted and performed a three  
50 dimensional reconstruction of the Z stack over time (see material and methods) to evaluate the  
51 dynamics of these foci at the nucleoid edge, we observed that excised foci moved rapidly on the  
52 surface of the nucleoid but keep nucleoid contact for most of their moves (Figure 6C). Deconvolution  
53 process allowed the transient resolution of 2 foci at the nucleoid edge, confirming that polar foci are  
54 frequently clusters of two or more excised circles. These results suggest that large DNA circles and  
55 plasmids lacking partition systems are expelled from the nucleoid core, in agreement with our  
56  
57  
58  
59  
60  
61  
62  
63  
64  
65

1 simulations, and find a home position at the nucleoid edge where they are free to surf on the  
2 nucleoid surface but cannot escape it. Excised circles might be unmixed from the nucleoid on the sole  
3 force of entropy but concomitantly they are maintained at the transition between the DNA  
4 compartment and the cytoplasm.  
5  
6  
7

## 8 **Localization and dynamics of R27 plasmid and excised circles when nucleoid and cell organization** 9 **are perturbed**

10  
11 Finally we tested if R27 and the DNA circle localizations at the nucleoid edge were maintained when  
12 chromosome confinement was changed. First, we used chloramphenicol to condense the nucleoid  
13 immediately after excision. We observed profound changes in the localization and dynamics of  
14 excised foci in these conditions (Figure 6D and 6E). The number of circle foci increased significantly (2  
15 to 3 per cell compared to 1 to 2 in the regular condition). The localization of these foci was changed,  
16 they were not only localized to the edge of the nucleoid, they were also observed on the side of the  
17 nucleoid. Even if the DNA free zone at the pole of the cell was enlarged by chloramphenicol  
18 treatment the excised circles did not explore it, they always kept contact with the nucleoid. Time-  
19 lapse experiments revealed that excised circle foci travel from the edge to the side of the nucleoid  
20 and vice versa (Figure 6E). In the presence of chloramphenicol, R27 plasmid localized to the side of  
21 the nucleoid and did not explore nucleoid free regions (Figure 6F). Similar results were observed with  
22 WT and  $\Delta$ parAB plasmids suggesting that chloramphenicol is altering the ParAB positioning system.  
23 These observations suggest that localization at the nucleoid pole is dependent on the volume  
24 occupied by the nucleoid or might eventually be created by transcription-translation-secretion  
25 (transertion) barriers (Roggiani & Goulian, 2015). We used cephalixin to block cell division and create  
26 large DNA free zones between segregated nucleoids. In these conditions filamenting cells presented  
27 multiple foci on the edge, the side and on the nucleoid (Figure 6G). The nucleoid-foci association was  
28 maintained for most cells. We only observed one focus crossing a nucleoid free space out of 200 cells  
29 monitored by timelapse over a 2h period (Figure 6G, right panel). These results confirmed that DNA  
30 circles lacking a partition system are unmixed from the chromosome but are maintained in the  
31 nucleoid space at the transition between the nucleoid and the cytoplasm.  
32  
33  
34  
35  
36  
37  
38  
39  
40  
41  
42  
43

## 44 **Discussion**

### 45 **Partition machinery and localization of plasmid**

46  
47 Our work extends to R27 the observation that plasmid lacking partition system are not localized with  
48 the nucleoid core. Using excised chromosomal circles and simulation we confirmed that this  
49 localization relies on the biophysical nature of large DNA circles in a crowded nucleoid and cytoplasm  
50 environment. Since the “natural” positioning of plasmids lacking partition systems is on the edge of  
51 the nucleoid, one could ask why partition systems do target plasmids inside the nucleoid? What  
52 could be the benefit for plasmid segregation to happen within the nucleoid? Could plasmid hijack  
53 entropy? In this scenario partition systems might serve as a localization system to the nucleoid to  
54 allow the plasmid to benefit from the entropic flow. Directionality will be given by protein-protein  
55 interactions and reaction-diffusion process of the ParB and ParA ATPase (Walter *et al*, 2017).  
56  
57  
58  
59  
60  
61  
62  
63  
64  
65

## How much plasmid DNA can be hosted in the nucleoid ?

Simulations indicate that for a define nucleoid volume the carrying capacity of plasmid DNA in the presence of a chromosome is limited. With the simulation parameters that we used, the normalized longitudinal spread of 700 kb plasmid reached that of the chromosome (Figure 5B). This limit is also observable in the frequency of nucleoid crossing that is extremely rare above 700 kb (Figure 6A). Above this size the plasmid, the nucleoid and perhaps cell morphology must adapt to this foreign DNA. Obviously this threshold is strictly dependent on the parameters that we used to defined the polymers. Changing the persistence length, the diameter of the chromatin cylinders or the nucleoid volume will modify these limits. Nevertheless, it is tempting to compare this 700 kb threshold with the size of plasmid and secondary chromosomes observed in bacteria. Every secondary replicon above 700 kb are secondary chromosomes. The presence of a large secondary replicon will therefore necessitate important chromosome conformation changes. Such changes could be detrimental and add an extra cost, in addition to the cost for replication and transcription, to secondary large replicons. Alternatively, the nucleoid volume might change to accommodate the extra replicon but this also has a significant cost in term of cell elongation for example.

The second critical size that we observed is much lower, under 200kb the probability to observe plasmid crossing the chromosome increased dramatically and the spread of plasmids approximate the values observed for plasmid residing in a chromosome free nucleoid shell. It is tempting to compare these values with the presence of segregation machinery encoded by plasmid genomes. Plasmids below 25-30 kb can cross the chromosome frequently and rapidly, ensuring efficient segregation by random partition. Above this value, the mobility of replicons becomes limiting and decrease exponentially with increasing size, rendering the presence of a positioning system required for stability. Above 200 kb, both the probability of crossing the chromosome and the crossing speed become extremely low, rendering compulsory the presence of a ParAB system, which is the only one of the three types of positioning systems ensuring both positioning of the replicons inside the nucleoid and separation of their sister copies after replication. Lastly, the presence of replicons above 700 kb in the nucleoid impact chromosome dynamics. These large replicons must thus adopt chromosome like behaviors. Consistent with this, the chromid of *V. cholerae* has an accurately regulated timing of replication, spreads in the long cell axis and couples segregation of its ter region with cell division as chromosomes do.

## Plasmid and excised circles are maintained at the nucleoid –cytoplasm transition

We observed that large plasmids and DNA circles lacking partition systems were expelled from their original localization toward nucleoid edges but did not invade the cytoplasmic space. This is in good agreement with our simulations suggesting that expulsion relates to entropic mediated unmixing of polymers in a confined space. However, entropy does not explain why these molecules do not invade large nucleoid free regions at the pole of the cell or in between nucleoids of filaments. One possible explanation for this could be that large circular DNA, differently, from small plasmid cannot diffuse in a glass-like cytoplasm (Parry *et al*, 2014). This has already been observed for other type of cytoplasm components that become disproportionally constrained with increasing size. Remarkably, small

1 plasmids lacking partition system appeared to diffuse rapidly within cytoplasm even when they form  
2 clusters (Reyes-Lamothe *et al*, 2014). A systematic analysis of plasmid or DNA circles mobility as a  
3 function of their size would be required to determine the critical size. However, we observed that  
4 DNA circles can slide rapidly on the surface of the nucleoid, this might suggest that the nature of the  
5 cytoplasm is not the only element contributing to their localization. Nucleic acid charges may also  
6 contribute to the control of diffusion at the transition between nucleoid and cytoplasm. Negatively  
7 charged ribosome surfaces may impose this limitation on the diffusion of proteins and DNA  
8 (Schavemaker *et al*, 2017). Interestingly the fluidity of the cytoplasm can be modulated by drugs  
9 affecting metabolism (Parry *et al*, 2014) or antimicrobial peptides (Zhu *et al*, 2019), our results  
10 suggest that plasmid localization and dynamics might also be affected by environmental conditions,  
11 this would influence their stability and expression and eventually change their cost for the host cell.  
12  
13  
14

### 15 **Could partition of genetic material imposes constrains on genome dynamics.**

16  
17  
18 In bacteria, horizontal gene transfer (HGT) is the main source of genome dynamics. Recent studies  
19 revealed that the size of horizontally acquired DNA in one single event is limited to 25-30kb (Pang &  
20 Lercher, 2017, 2019). Plasmids and lysogenic phages are the main drivers of HGT. Interestingly this 25  
21 kb limit also corresponds to the presence of partition systems on plasmids. Our simulations show  
22 that the ability of plasmid to cross the nucleoid is exponentially decreasing with increasing size  
23 (Figure 5). Experiment with R27 plasmid or excised circles clearly show that nucleoid crossing is very  
24 rare for 130 kb -200 kb DNA circles. Entropic unmixing might therefore limit the ability of a newly  
25 acquired replicon to find a target sequence for integration. In good agreement with this hypothesis it  
26 appeared that DNA internal motion likely accelerates protein target search in a packed nucleoid  
27 (Chow & Skolnick, 2017)  
28  
29  
30  
31  
32  
33

## 34 **Material and methods**

### 35 **Annotation of subcellular positioning systems**

36  
37  
38  
39 Partition systems ParAB and ParMR were detected using HMM profiles used in our previous work  
40 (Cury *et al*, 2017). Briefly, systems were reported when the two hits of a given system were  
41 contiguous in the replicon. A hit was considered significant if the e-value was smaller than  $10^{-3}$  and  
42 the coverage of the profile was above 50%. For annotation of *stbA*, tBLASTN searches were  
43 performed against the 971 plasmids using the *stbA* sequences previously reported (Guynet *et al*,  
44 2011). Each plasmid with a positive result was annotated in SnapGene. oriTDB  
45 (<http://202.120.12.134/oriTfinder/oriTfinder.html>)  
46 was used to determine possible *oriT* site, relaxases and type IV secretion system genes. We found a  
47 *stbA* or *stbA* like sequence in 136 plasmids (Figure 1). To further annotate plasmids with no detected  
48 systems, *parA* and *parM* genes were searched using tBLASTN in the 79 plasmids without segregation  
49 system after the automatic annotation of *ParA* and *ParM* and the *StbA* annotation. We used the  
50 *parA* sequence found in NC\_012961, the *parM* sequences described by Jakob Møller-Jensen and colleagues  
51 (van den Ent *et al*, 2002) and the *parM* sequence of JCW3 (*Clostridium perfringens*). Using this strategy,  
52 we found 54 plasmids with a *parA*-like sequence (including 5 with a frameshift and 1 partial sequence) and  
53 6 plasmids with *parM*-like sequence (including 3 with a frameshift).  
54  
55  
56  
57  
58  
59  
60  
61  
62  
63  
64  
65

1 The 19 remaining plasmid sequences with no system detected were all annotated in SnapGene and  
2 inspected “by eyes”. Two sequences were obviously partial sequences of larger plasmids. Mobile  
3 genetics elements (MGE) were annotated using ISfinder (<https://www-is.biotoul.fr/>)(Siguier *et al*,  
4 2006), bacteriophage with PHASTER (<http://phaster.ca/>)(Arndt *et al*, 2016). Four plasmids carried  
5 ribosomal operons, others were mostly constituted by MGE or bacteriophages.  
6

## 7 **Strains and plasmids**

8  
9 R27 is a 180 kb plasmid of the IncHI family, naturally resistant to tetracycline (Phan & Wain, 2008;  
10 Lawley & Taylor, 2003). We detected a potential toxin-antitoxin system consisting of gene *stm* and an  
11 upstream RNA, which we deleted from positions 91,174 to 91,481 bp on the R27 sequence and  
12 replaced by the *lacI* gene. For intracellular localization, we inserted a P1 *parS*-Kn cassette (Stouf *et al*,  
13 2013) in the intergenic region between the two converging genes R149 and R150 (position 138,435).  
14 The ParAB and ParRM systems (R0019-R0020 and R0013-StbA, respectively) were deleted from the  
15 beginning of the first gene to the end of the second gene (23,081 to 25,338 and 18,079 to 19,834,  
16 respectively), replaced by a FRT-Kn-FRT cassette that was subsequently resolved to remove the KnR  
17 determinant. Note that the ParM homolog is called StbA in R27 annotation but is not a StbA  
18 homolog. R27 derivatives were introduced into a  $\Delta(lacI)$  strain (Deghorain *et al*, 2011) for stability  
19 assays and in a  $\Delta(lacZ)::gfp-parBP1$  strain (Stouf *et al*, 2013) for microscopy. For the excision of the  
20 137 kb we used the FBG150 *trkD*<sup>attL</sup> R719 strain (Valens *et al*, 2016) containing attL from  $\lambda$  at the *trkD*  
21 locus (3928826 bp) and attR at the position 4067141bp. Excision is produced by the Int and Xis  
22 protein from I produced from the plasmid pTSA29-CXI (Valens *et al*, 2004). The *parS* P1 tag was  
23 inserted at the Ori-7 position at 4024865 bp.  
24  
25  
26  
27  
28  
29  
30

31 **Imaging of excised DNA circle and R27.** Excision was obtained as described before (Valens *et al*,  
32 2016) with a 30 min heat shock at O.D. 0.1. Bacteria were immediately spread on M9-casaminoacids  
33 and glucose agarose pad supplemented or not with chloramphenicol (30  $\mu$ g/ml). When required,  
34 cephalixin (20 $\mu$ g/ml) was added to the culture medium 1 h before heat shock. Imaging was  
35 performed on a Zeiss inverted microscope equipped with a Yokogawa W1 spinning disk head and an  
36 Orca-Flash 4 CMOS camera. The incubation is maintained to 30°C during imaging. Time-lapse  
37 acquisition was controlled by Metamorph software. Deconvolution was performed with Huygens and  
38 3D reconstruction with Imaris softwares. Image analysis was performed with Object J (Vischer *et al*,  
39 2015), Microbe-J (Ducret *et al*, 2016), Track-mate (Tinevez *et al*, 2017) and Particle Tracker  
40 (Sbalzarini & Koumoutsakos, 2005).  
41  
42  
43  
44  
45  
46  
47

48 **Simulations.** We simulated *E. coli* chromosomes using a worm-like chain (WLC) model, i.e. a flexible  
49 fiber model, of the bacterial chromosome (Junier *et al*, 2014; Lepage & Junier, 2017). One  
50 chromosomes and one plasmid were embedded in a volume whose dimensions corresponded to the  
51 nucleoid that is observed *in vivo*: a diameter equal to 800 nm and a length from 2.0  $\mu$ m (G1 phase).  
52 We excluded the possibility of the fibers to overlap (self-avoidance constraint) by using hard-core  
53 diameters of the nucleoproteic fiber of 35 nm. The base-pair density along the fiber was fixed at 100  
54 bp/nm and the persistence length at 100 nm, a value that is much smaller than the diameter of the  
55 nucleoid. Simulations and thermodynamic analysis were performed as described previously (Junier *et al*,  
56 2014). Briefly the chromosome and plasmid consisted of a semi-flexible polymer composed of a  
57 succession of *N* impenetrable cylinders (three cylinders per persistence length)—*N* = 1392 for the 4.6  
58  
59  
60  
61  
62  
63  
64  
65

1 Mb chromosome. The state space of our polymer models was sampled using a standard Monte–Carlo  
2 procedure (Metropolis accept/rejection rule). For each plasmid we performed three simulations (two  
3 in the presence of the chromosome and one in its absence). Each simulation consisted of two stages:  
4 (i) an initialization stage (see above) and (ii) a thermodynamic analysis. The initial polymer  
5 conformations were obtained by first equilibrating the system in the presence of all forces and  
6 without confinement (large initial embedding volume). The cell volume was next slowly reduced  
7 down to the nucleoid volume, and the thermodynamic properties were eventually computed. The  
8 slow reduction of the embedding volume aimed at ensuring that the conformations were the most  
9 likely from a thermodynamic point of view (by preventing as much as possible the formation of long-  
10 living metastable kinetic conformations). The X, Y, Z position of each plasmid and chromosome  
11 monomer and the barycenter of the replicon were recorded every 15 000 iterations (Figure 2A).  
12  
13  
14  
15  
16  
17

## 18 Acknowledgements

19 We thank Stephane Duigou, Michele Valens and Frédéric Boccard for the gift of strains and technical  
20 advices for DNA excisions. We thank members of Orion, the CIRB imaging facility. We are deeply  
21 thankful to Thibault Lepage for his help on setting up the simulations. This work as funded by ANR  
22 ANR-14-CE10-0007-01 to OE, FC and ER by the CNRS PICS initiative to OE and IJ and by the  
23 Foundation ARC (PJA 20171206119) to OE.  
24  
25  
26  
27  
28  
29

## 30 References

- 31 Arndt D, Grant JR, Marcu A, Sajed T, Pon A, Liang Y & Wishart DS (2016) PHASTER: a better, faster  
32 version of the PHAST phage search tool. *Nucleic Acids Res.* **44**: W16-21  
33  
34 Baltrus DA (2013) Exploring the costs of horizontal gene transfer. *Trends Ecol. Evol.* **28**: 489–495  
35  
36 Bouet J-Y & Funnell BE (2019) Plasmid Localization and Partition in Enterobacteriaceae. *EcoSal Plus* **8**:  
37  
38 Bouma JE & Lenski RE (1988) Evolution of a bacteria/plasmid association. *Nature* **335**: 351–352  
39  
40 Carroll AC & Wong A (2018) Plasmid persistence: costs, benefits, and the plasmid paradox. *Can. J.*  
41 *Microbiol.* **64**: 293–304  
42  
43 Cass JA, Kuwada NJ, Traxler B & Wiggins PA (2016) Escherichia coli Chromosomal Loci Segregate from  
44 Midcell with Universal Dynamics. *Biophys. J.* **110**: 2597–2609  
45  
46 Chow E & Skolnick J (2017) DNA Internal Motion Likely Accelerates Protein Target Search in a Packed  
47 Nucleoid. *Biophys. J.* **112**: 2261–2270  
48  
49 Cury J, Touchon M & Rocha EPC (2017) Integrative and conjugative elements and their hosts:  
50 composition, distribution and organization. *Nucleic Acids Res.* **45**: 8943–8956  
51  
52 Deghorain M, Pagès C, Meile J-C, Stouf M, Capiaux H, Mercier R, Lesterlin C, Hallet B & Cornet F  
53 (2011) A defined terminal region of the E. coli chromosome shows late segregation and high  
54 FtsK activity. *PloS One* **6**: e22164  
55  
56  
57  
58  
59  
60  
61  
62  
63  
64  
65



- 1 Derman AI, Lim-Fong G & Pogliano J (2008) Intracellular mobility of plasmid DNA is limited by the  
2 ParA family of partitioning systems. *Mol. Microbiol.* **67**: 935–946
- 3 Ducret A, Quardokus EM & Brun YV (2016) MicrobeJ, a tool for high throughput bacterial cell  
4 detection and quantitative analysis. *Nat. Microbiol.* **1**: 16077
- 5  
6 van den Ent F, Møller-Jensen J, Amos LA, Gerdes K & Löwe J (2002) F-actin-like filaments formed by  
7 plasmid segregation protein ParM. *EMBO J.* **21**: 6935–6943
- 8  
9 Erdmann N, Petroff T & Funnell BE (1999) Intracellular localization of P1 ParB protein depends on  
10 ParA and parS. *Proc. Natl. Acad. Sci. U. S. A.* **96**: 14905–14910
- 11  
12 Gordon GS, Sitnikov D, Webb CD, Teleman A, Straight A, Losick R, Murray AW & Wright A (1997)  
13 Chromosome and low copy plasmid segregation in *E. coli*: visual evidence for distinct  
14 mechanisms. *Cell* **90**: 1113–1121
- 15  
16  
17 Guynet C, Cuevas A, Moncalián G & de la Cruz F (2011) The *stb* operon balances the requirements for  
18 vegetative stability and conjugative transfer of plasmid R388. *PLoS Genet.* **7**: e1002073
- 19  
20  
21 Harrison PW, Lower RPJ, Kim NKD & Young JPW (2010) Introducing the bacterial ‘chromid’: not a  
22 chromosome, not a plasmid. *Trends Microbiol.* **18**: 141–148
- 23  
24  
25 Ho TQ, Zhong Z, Aung S & Pogliano J (2002) Compatible bacterial plasmids are targeted to  
26 independent cellular locations in *Escherichia coli*. *EMBO J.* **21**: 1864–1872
- 27  
28  
29 Jun S & Mulder B (2006) Entropy-driven spatial organization of highly confined polymers: Lessons for  
30 the bacterial chromosome. *Proc. Natl. Acad. Sci.* **103**: 12388–12393
- 31  
32 Junier I, Boccard F & Espéli O (2014) Polymer modeling of the *E. coli* genome reveals the involvement  
33 of locus positioning and macrodomain structuring for the control of chromosome  
34 conformation and segregation. *Nucleic Acids Res.* **42**: 1461–1473
- 35  
36  
37 Lawley TD & Taylor DE (2003) Characterization of the double-partitioning modules of R27: correlating  
38 plasmid stability with plasmid localization. *J. Bacteriol.* **185**: 3060–3067
- 39  
40  
41 Le Gall A, Cattoni DI, Guilhas B, Mathieu-Demazière C, Oudjedi L, Fiche J-B, Rech J, Abrahamsson S,  
42 Murray H, Bouet J-Y & Nollmann M (2016) Bacterial partition complexes segregate within the  
43 volume of the nucleoid. *Nat. Commun.* **7**: 12107
- 44  
45 Lepage T & Junier I (2017) Modeling Bacterial DNA: Simulation of Self-Avoiding Supercoiled Worm-  
46 Like Chains Including Structural Transitions of the Helix. *Methods Mol. Biol. Clifton NJ* **1624**:  
47 323–337
- 48  
49 Marchetti M, Capela D, Glew M, Cruveiller S, Chane-Woon-Ming B, Gris C, Timmers T, Poinso V,  
50 Gilbert LB, Heeb P, Médigue C, Batut J & Masson-Boivin C (2010) Experimental evolution of a  
51 plant pathogen into a legume symbiont. *PLoS Biol.* **8**: e1000280
- 52  
53  
54 Niki H & Hiraga S (1997) Subcellular distribution of actively partitioning F plasmid during the cell  
55 division cycle in *E. coli*. *Cell* **90**: 951–957
- 56  
57  
58 Pang TY & Lercher MJ (2017) Supra-operonic clusters of functionally related genes (SOCs) are a  
59 source of horizontal gene co-transfers. *Sci. Rep.* **7**: 40294
- 60  
61  
62  
63  
64  
65

- 1 Pang TY & Lercher MJ (2019) Each of 3,323 metabolic innovations in the evolution of *E. coli* arose  
2 through the horizontal transfer of a single DNA segment. *Proc. Natl. Acad. Sci. U. S. A.* **116**:  
3 187–192
- 4 Parry BR, Surovtsev IV, Cabeen MT, O’Hern CS, Dufresne ER & Jacobs-Wagner C (2014) The bacterial  
5 cytoplasm has glass-like properties and is fluidized by metabolic activity. *Cell* **156**: 183–194  
6
- 7 Phan M-D & Wain J (2008) IncHI plasmids, a dynamic link between resistance and pathogenicity. *J.*  
8 *Infect. Dev. Ctries.* **2**: 272–278  
9
- 10 Ramachandran R, Jha J, Paulsson J & Chattoraj D (2017) Random versus Cell Cycle-Regulated  
11 Replication Initiation in Bacteria: Insights from Studying *Vibrio cholerae* Chromosome 2.  
12 *Microbiol. Mol. Biol. Rev. MMBR* **81**:  
13
- 14 Reyes-Lamothe R, Tran T, Meas D, Lee L, Li AM, Sherratt DJ & Tolmasky ME (2014) High-copy  
15 bacterial plasmids diffuse in the nucleoid-free space, replicate stochastically and are  
16 randomly partitioned at cell division. *Nucleic Acids Res.* **42**: 1042–1051  
17
- 18 Roggiani M & Goulian M (2015) Chromosome-Membrane Interactions in Bacteria. *Annu. Rev. Genet.*  
19 **49**: 115–129  
20
- 21 Sbalzarini IF & Koumoutsakos P (2005) Feature point tracking and trajectory analysis for video  
22 imaging in cell biology. *J. Struct. Biol.* **151**: 182–195  
23
- 24 Schavemaker PE, Śmigiel WM & Poolman B (2017) Ribosome surface properties may impose limits on  
25 the nature of the cytoplasmic proteome. *eLife* **6**:  
26
- 27 Sengupta M, Nielsen HJ, Youngren B & Austin S (2010) P1 plasmid segregation: accurate  
28 redistribution by dynamic plasmid pairing and separation. *J. Bacteriol.* **192**: 1175–1183  
29
- 30 Siguier P, Perochon J, Lestrade L, Mahillon J & Chandler M (2006) ISfinder: the reference centre for  
31 bacterial insertion sequences. *Nucleic Acids Res.* **34**: D32-36  
32
- 33 Smillie C, Garcillán-Barcia MP, Francia MV, Rocha EPC & de la Cruz F (2010) Mobility of plasmids.  
34 *Microbiol. Mol. Biol. Rev. MMBR* **74**: 434–452  
35
- 36 Stouf M, Meile J-C & Cornet F (2013) FtsK actively segregates sister chromosomes in *Escherichia coli*.  
37 *Proc. Natl. Acad. Sci. U. S. A.* **110**: 11157–11162  
38
- 39 Taylor DE (1983) Transfer-defective and tetracycline-sensitive mutants of the incompatibility group  
40 HI plasmid R27 generated by insertion of transposon 7. *Plasmid* **9**: 227–239  
41
- 42 Tinevez J-Y, Perry N, Schindelin J, Hoopes GM, Reynolds GD, Laplantine E, Bednarek SY, Shorte SL &  
43 Eliceiri KW (2017) TrackMate: An open and extensible platform for single-particle tracking.  
44 *Methods San Diego Calif* **115**: 80–90  
45
- 46 Valens M, Penaud S, Rossignol M, Cornet F & Boccard F (2004) Macrodomain organization of the  
47 *Escherichia coli* chromosome. *EMBO J.* **23**: 4330–4341  
48
- 49 Valens M, Thiel A & Boccard F (2016) The MaoP/maoS Site-Specific System Organizes the Ori Region  
50 of the *E. coli* Chromosome into a Macrodomain. *PLoS Genet.* **12**: e1006309  
51  
52  
53  
54  
55  
56  
57  
58  
59  
60  
61  
62  
63  
64  
65

1 Vischer NOE, Verheul J, Postma M, van den Berg van Saparoea B, Galli E, Natale P, Gerdes K, Luirink J,  
2 Vollmer W, Vicente M & den Blaauwen T (2015) Cell age dependent concentration of  
3 Escherichia coli divisome proteins analyzed with ImageJ and ObjectJ. *Front. Microbiol.* **6**: 586  
4  
5 Vologodskii AV & Cozzarelli NR (1993) Monte Carlo analysis of the conformation of DNA catenanes. *J.*  
6 *Mol. Biol.* **232**: 1130–1140  
7  
8 Vologodskii AV, Levene SD, Klenin KV, Frank-Kamenetskii M & Cozzarelli NR (1992) Conformational  
9 and thermodynamic properties of supercoiled DNA. *J. Mol. Biol.* **227**: 1224–1243  
10  
11 Walter J-C, Dorignac J, Lorman V, Rech J, Bouet J-Y, Nollmann M, Palmeri J, Parmeggiani A & Geniet F  
12 (2017) Surfing on Protein Waves: Proteophoresis as a Mechanism for Bacterial Genome  
13 Partitioning. *Phys. Rev. Lett.* **119**: 028101  
14  
15  
16 Zhu Y, Mohapatra S & Weisshaar JC (2019) Rigidification of the Escherichia coli cytoplasm by the  
17 human antimicrobial peptide LL-37 revealed by superresolution fluorescence microscopy.  
18 *Proc. Natl. Acad. Sci. U. S. A.* **116**: 1017–1026  
19  
20  
21  
22  
23  
24

## 25 Legend of the figures

27 **Figure 1. A)** Distribution of subcellular positioning systems in enterobacterial secondary replicons. 970  
28 replicons were ranked according to their size (x-axis; the top panel shows a cumulative plot of  
29 replicon sizes indicative of size density). The bottom four panels show event plots of the indicated  
30 system (vertical line indicates presence of the indicated system) or absence of system detected  
31 (none). B) Localization of the R27, R27  $\Delta$ parAB, R27  $\Delta$ parRM plasmids (parS/parBGFP, green) and  
32 nucleoid (Hu-mCherry, red) C) Localization along the long axis of the *E. coli* cell of the R27 tagged  
33 with a parS/ParB-GFP tag. Cells with one focus of the WT R27, R27 delta parAB, R27 delta parRM (N  
34 =1000). D) Distribution of R27 localization as in C for cells with two R27 foci.

38  
39 **Figure 2. A)** Description of the in silico simulation of plasmid and chromosome and the main  
40 parameters that we collected during the simulations. B) In silico simulation of the localization pattern  
41 of plasmids (green circles) and chromosome edges (red traces) along the longitudinal axis of the  
42 nucleoid . Plasmid size (Lp) ranging from 30 kb to 1000 kb are represented. The simulations were run  
43 for at least  $3 \times 10^7$  iterations.

44  
45  
46 **Figure 3. A)** In silico simulations of the localization of plasmid barycenter along the longitudinal axis  
47 of the nucleoid (histograms) and the short axes of the nucleoid (scatter plot). The barycenter of the  
48 chromosome is plotted in red on the scatter plots. The black ovoid line map the position of the 70 kb  
49 plasmid the most distant from the cell center, the same line is drawn on the 600kb scatter plot to  
50 illustrate the fact that barycenters of large plasmids are more frequently localized toward nucleoid  
51 center. B) Examples of 600 kb plasmid (green polymer) localization according to the positioning of its  
52 barycenter along the longitudinal axis of the nucleoid. Plasmids crossing chromosomes (purple  
53 polymer) tend to occupy the lateral side of the nucleoid. C) Histograms of the localization of 200 kb  
54 and 600kb plasmid barycenters.  
55  
56  
57  
58  
59  
60  
61  
62  
63  
64  
65

**Figure 4.** A) Analyzes of plasmid and chromosome spatial extension along the longitudinal axis (Zspread) of the cell. Red circle represent the median chromosome extension according to the size of the plasmid present in the same nucleoid. The green circles represent the extension of the plasmid in the presence of a chromosome. Open green circles represent the extension of plasmid in an empty nucleoid shell. Data were fitted with power laws. B) Normalized spreading (NS) of plasmids and chromosome along the longitudinal axis of the nucleoid.  $NS = Zspread / \text{Size of the replicon (kb)}$ . Data were fitted with power laws. C) Frequency of plasmid crossing events according to plasmid size. Data were fitted by a double exponential decay  $[\text{Freq crossing}] = 25 * e^{(-0.03 * Lp)} + 9 * e^{(-0.004 * Lp)}$ ;  $R^2 = 0.98$ . D) Average speed of chromosome crossing for small plasmids. Data were fitted by a double exponential decay  $[\text{Crossing speed}] = 1822 * e^{(-0.15 * Lp)} + 12 * e^{(-0.007 * Lp)}$ ;  $R^2 = 0.99$ . E) Traces of the 200 kb plasmid simulation. The positioning of a plasmid locus (green) and a chromosome locus (red) were represented. The velocity of movement of the loci along the longitudinal axis of the nucleoid is measured for crossing events of the plasmid (orange lines) and the chromosome (black lines). The average velocity of the detected crossing events was plotted. F) Distribution of mobility of plasmid loci at the polar position (longitudinal position  $<500 \text{ nm}$  or  $>1500 \text{ nm}$ ). The 3D displacement of the locus is measured for 15 000 iteration intervals.

**Figure 5.** A) Examples of the localization of the *parS*/ParB-GFP foci (green) at the Ori-7 position of the chromosome (top) and on a 117 kb excised circle (bottom). The nucleoid is labeled with the HU-mCherry fusion (red). The positioning of *parS*/ParB-GFP foci according to cell size were recorded before or 1h after induction of the Xis and Int recombinase to promote excision. B) Kymographs representing the movement of *parS*/ParB-GFP foci at the chromosomal locus, on the excised circle, R27 and R27  $\Delta$ *parAB* plasmids. Duration and frame intervals are indicated on top of each kymograph. C) Montage of a representative ballistic movement of the excised circle. D) Mean Squared Displacement analysis of *parS*/ParB-GFP focus at the chromosomal location or on the 117 kb excised circle. E) Log –Log representation of the MSD analysis presented in D. Power law fitting of the data  $MSD = D * \Delta T^\alpha$ . F) Mean Squared Displacement analysis of *parS*/ParB-GFP focus on the R27 and R27  $\Delta$ *parAB* plasmids. E) Log –Log representation of the MSD analysis presented in F Power law fitting of the data  $MSD = D * \Delta T^\alpha$ .

**Figure 6.** A) Average normalized fluorescence intensity of *parS*/ParB-GFP foci on excised circles and nucleoid labeled with HU-mCherry along the longitudinal axis of the cell. Cell border is determined as the half maximum of the phase contrast signal. B) Lateral and longitudinal displacements (60 x 120 sec) of an excised *parS*/ParB-GFP focus at the nucleoid edge. The nucleoid (red shade) is drawn for illustration, its exact contour changes from frame to frame. C) 3D timelapse imaging of the movement of excised foci at the edge of the nucleoid. Imaging was of *parS*/ParB-GFP and HU-mCherry was performed with 5 Z planes (interval 200 nm each) at 20 second intervals. Images were deconvoluted and 3D reconstructed. D) Examples of the localization of the *parS*/ParB-GFP foci (green) on a 117 kb excised circle in the presence of chloramphenicol to condense the nucleoid (HU-mCherry, Red). The arrow indicates the movement of excised foci toward lateral edges of the nucleoid. Right panel, kymograph along the longitudinal axis of the cell marked with the arrow. E) Same as in A with a shorter imaging time interval (6 sec). Movement of excised foci toward lateral edges of the nucleoid is also observable at this time scale. Kymograph (along the white line) showing the movement of the polar *parS*/ParB-GFP foci toward the cell center via nucleoid edges. F) Localization of the R27 and R27  $\Delta$ *parAB* in the presence of chloramphenicol. G) Examples of the localization of the *parS*/ParB-GFP foci (green) on a 117 kb excised circle in the presence of

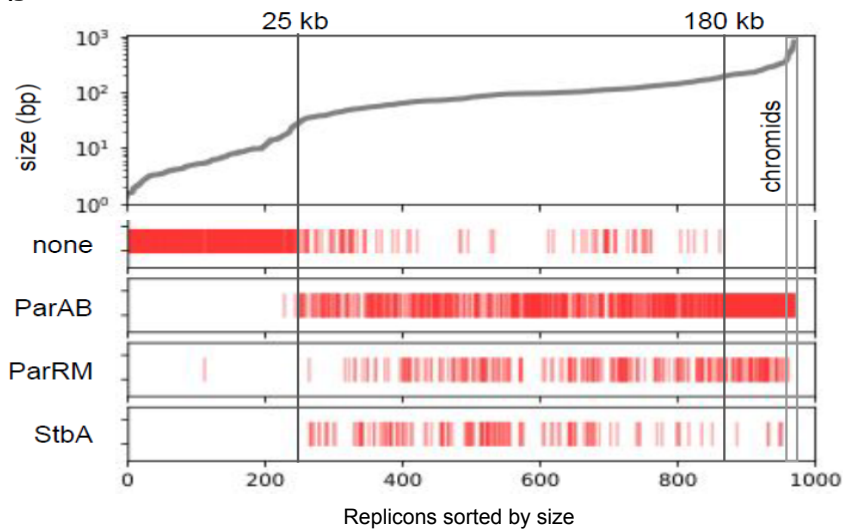
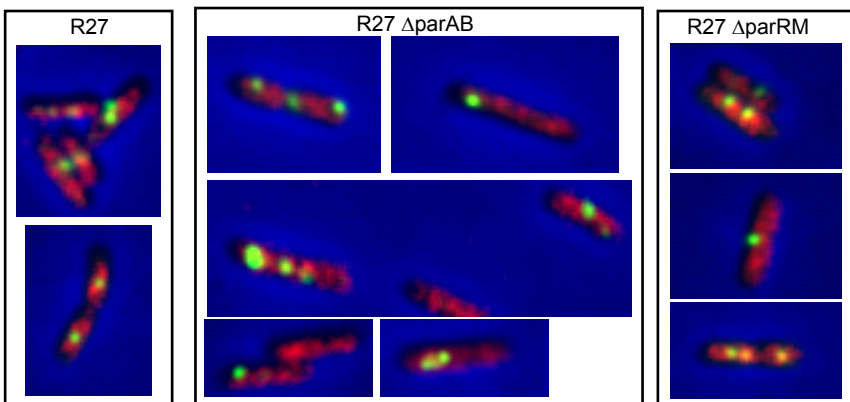
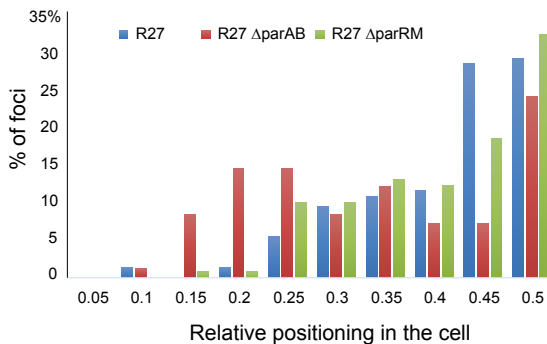
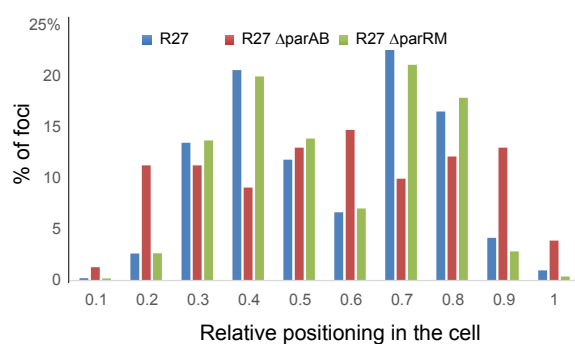
1 cephalixin to block division and create large cytoplasmic regions in between nucleoids (HU-mCherry,  
2 Red). The arrow on the right panel indicates the only parS/ParB-GFP focus crossing the cytoplasmic  
3 space observed among 200 cells.  
4  
5  
6

### 7 **Legend of the supplementary figures**

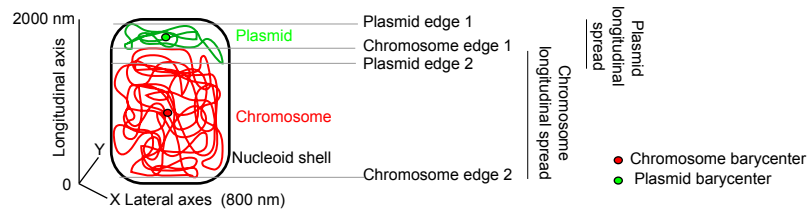
8  
9 **Supplementary Figure S1.** Measure of the rate of loss of R27, R27  $\Delta$ parAB and R27  $\Delta$ parMR plasmids  
10

11 **Supplementary Figure S2.** A) Traces of the positioning along the longitudinal axis of the nucleoid of a  
12 200 kb plasmid in the presence (green dots) or absence of chromosome (blue circles) within the  
13 nucleoid. B) Distribution of the positioning of the 200 kb plasmid along the longitudinal axis of the  
14 nucleoid in the presence (green) or absence (orange) of the chromosome. C) Distribution of the  
15 positioning of the 200 kb plasmid along lateral axis of the nucleoid in the presence (green) or  
16 absence (orange) of the chromosome. D) Traces of the positioning along the longitudinal axis of the  
17 nucleoid of a 600 kb plasmid in the presence (green dots) or absence of chromosome (blue circles)  
18 within the nucleoid. E) Distribution of the positioning of the 600 kb plasmid along the longitudinal  
19 axis of the nucleoid in the presence (green) or absence (orange) of the chromosome. F) Distribution  
20 of the positioning of the 600 kb plasmid along lateral axis of the nucleoid in the presence (green) or  
21 absence (orange) of the chromosome.  
22  
23  
24  
25  
26

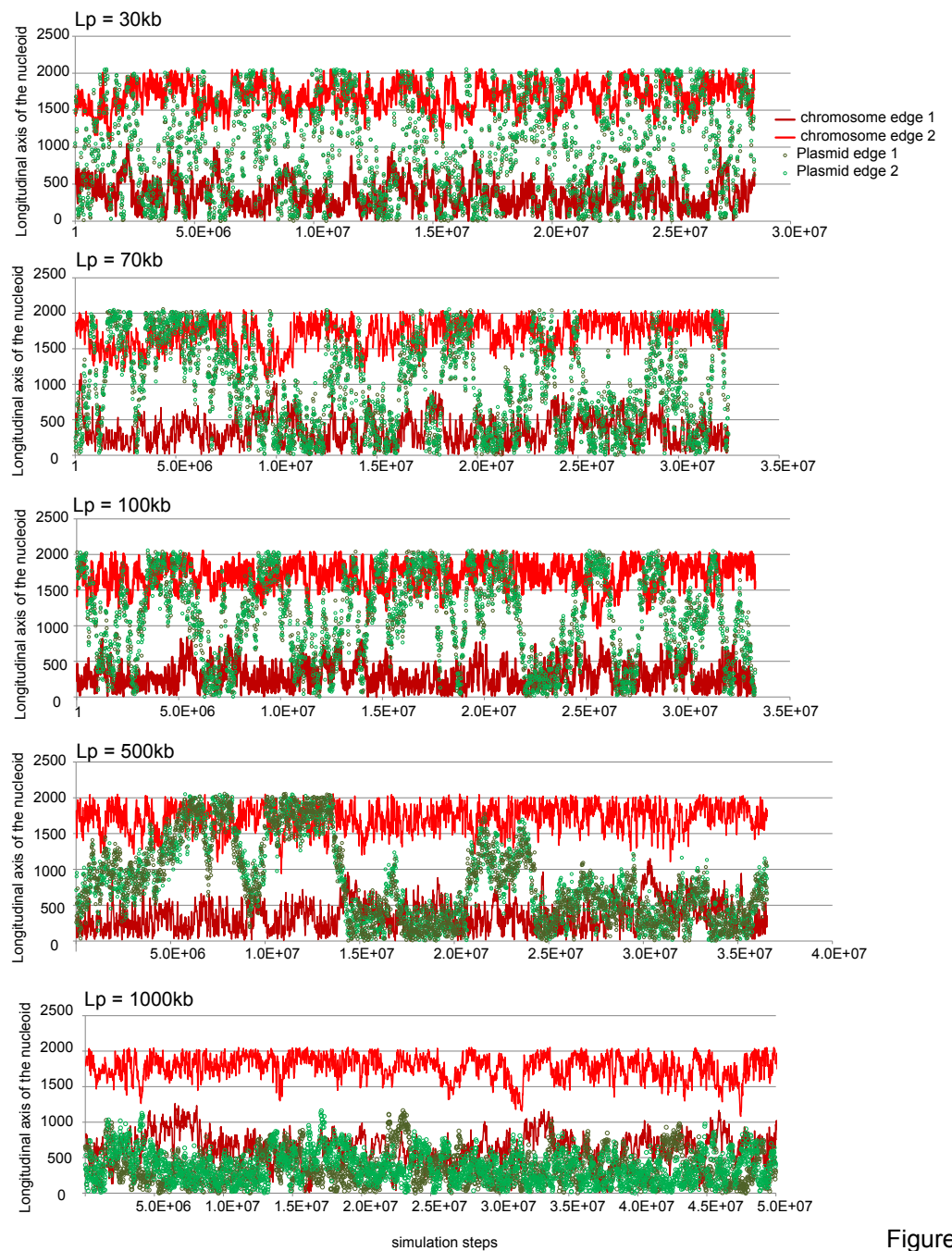
27 **Supplementary Figure S3.** A) Distribution of the 200kb plasmid spatial extension along the  
28 longitudinal axis of the nucleoid according to the positioning of its barycenter in the presence of a  
29 chromosome. B) Distribution of the 200kb plasmid spatial extension along the longitudinal axis of  
30 the nucleoid according to the positioning of its barycenter in the absence of a chromosome. C)  
31 Distribution of the 200kb plasmid spatial extension along the lateral axis of the nucleoid according to  
32 the positioning of its barycenter in the presence of a chromosome. B) Distribution of the 200kb  
33 plasmid spatial extension along the lateral axis of the nucleoid according to the positioning of its  
34 barycenter in the absence of a chromosome.  
35  
36  
37  
38  
39  
40  
41  
42  
43  
44  
45  
46  
47  
48  
49  
50  
51  
52  
53  
54  
55  
56  
57  
58  
59  
60  
61  
62  
63  
64  
65

**Figure 1****B****C****D**

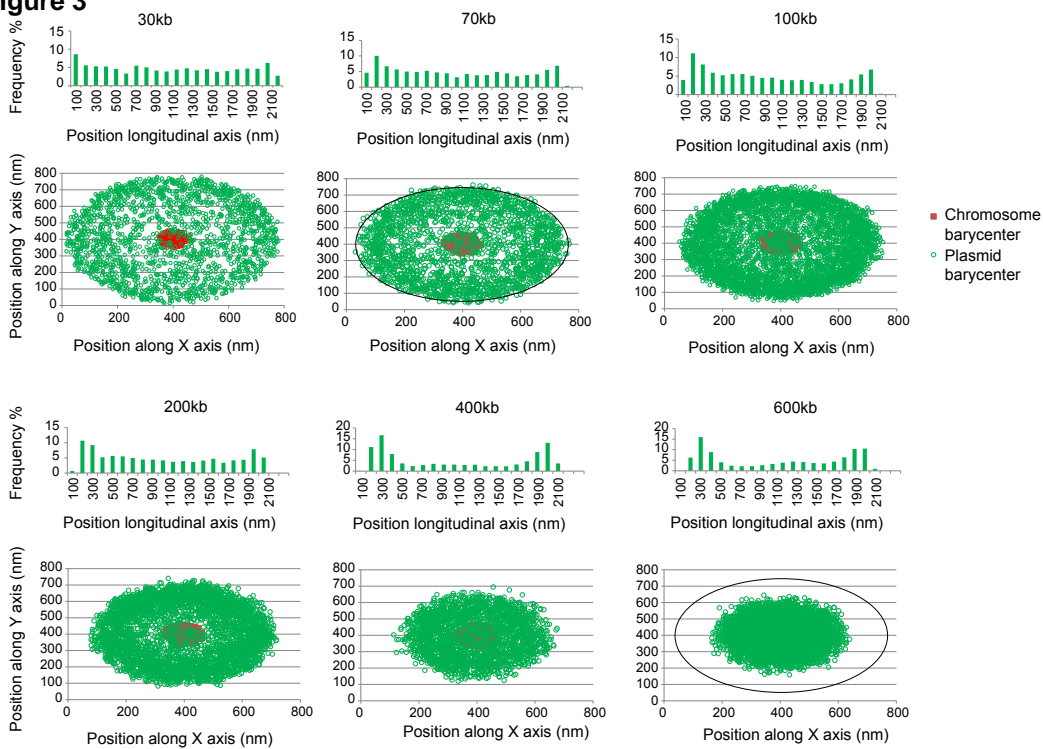
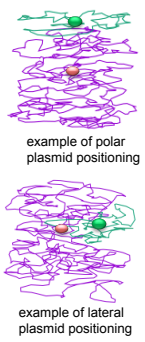
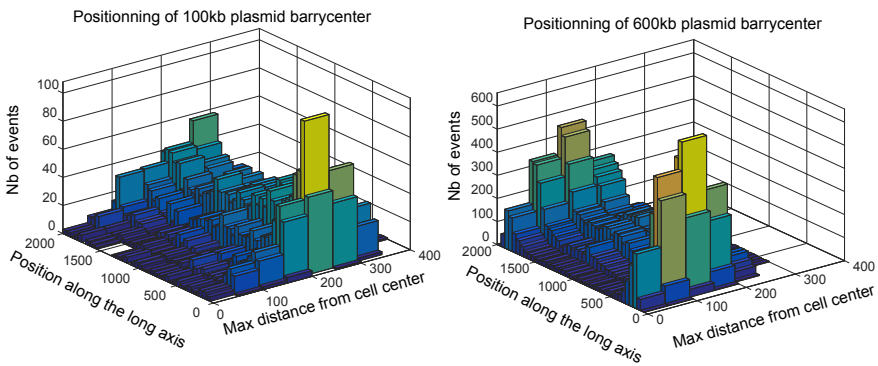
**Figure 2**



**B**



**Figure 2**

**Figure 3****B****C****Figure 3**



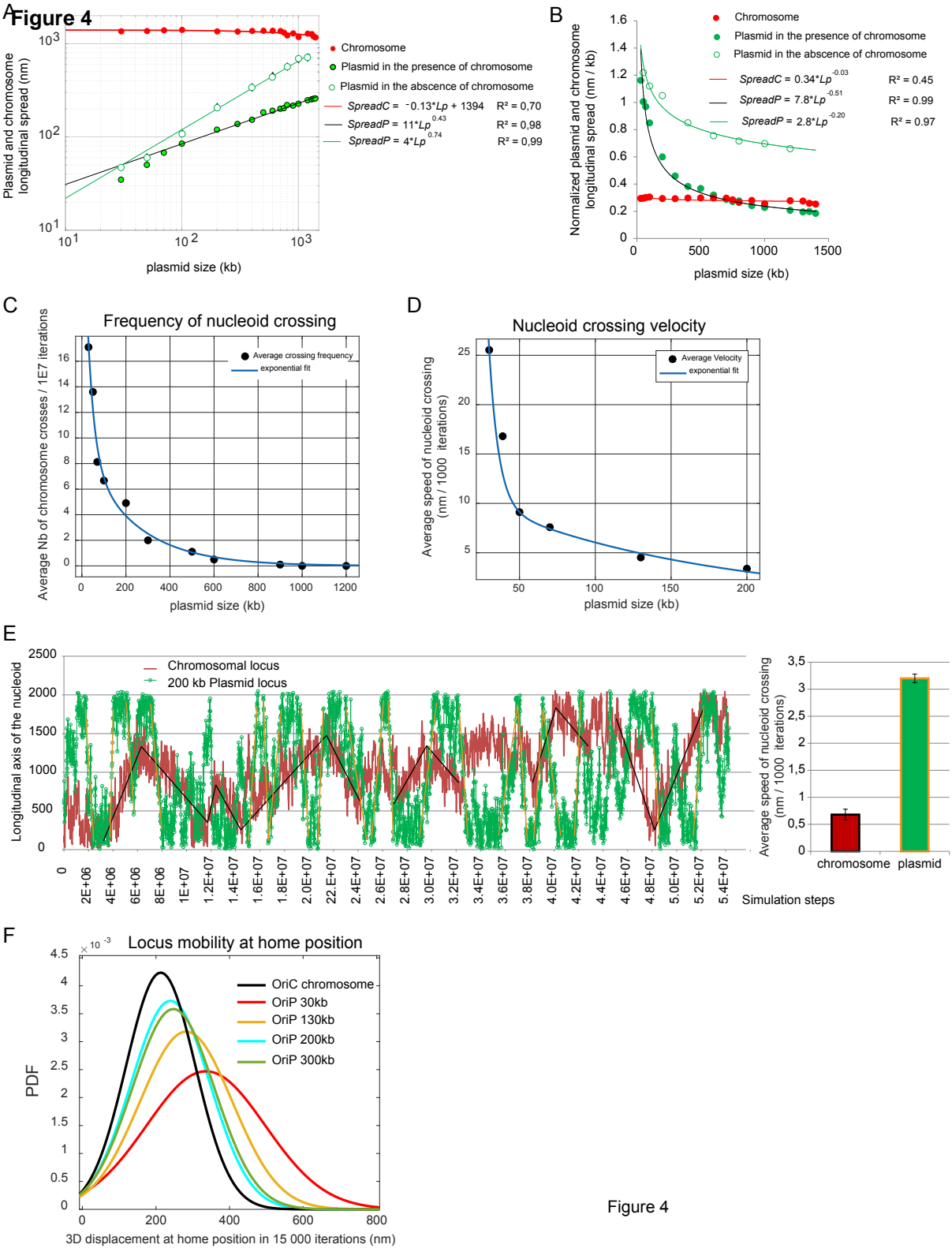
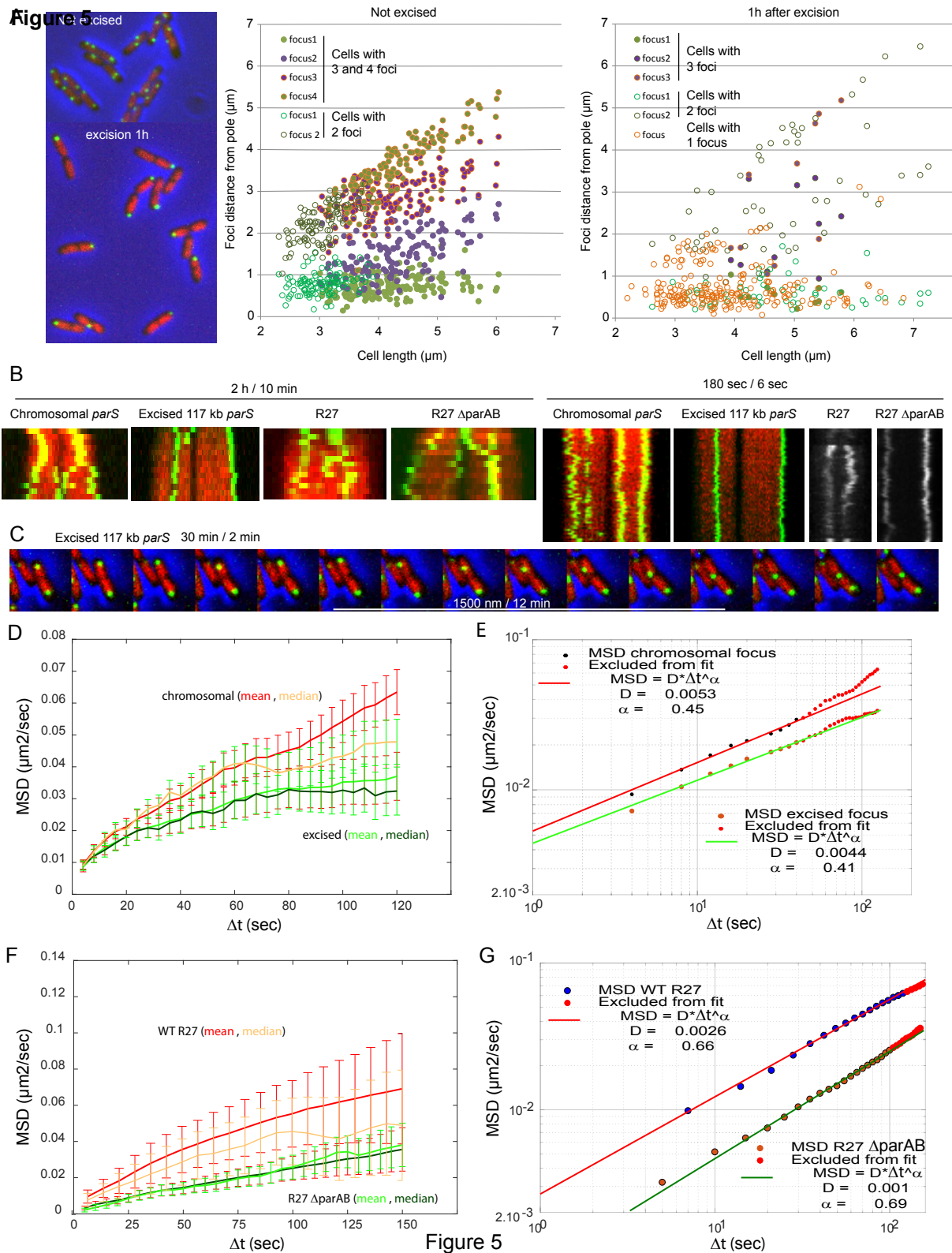


Figure 4



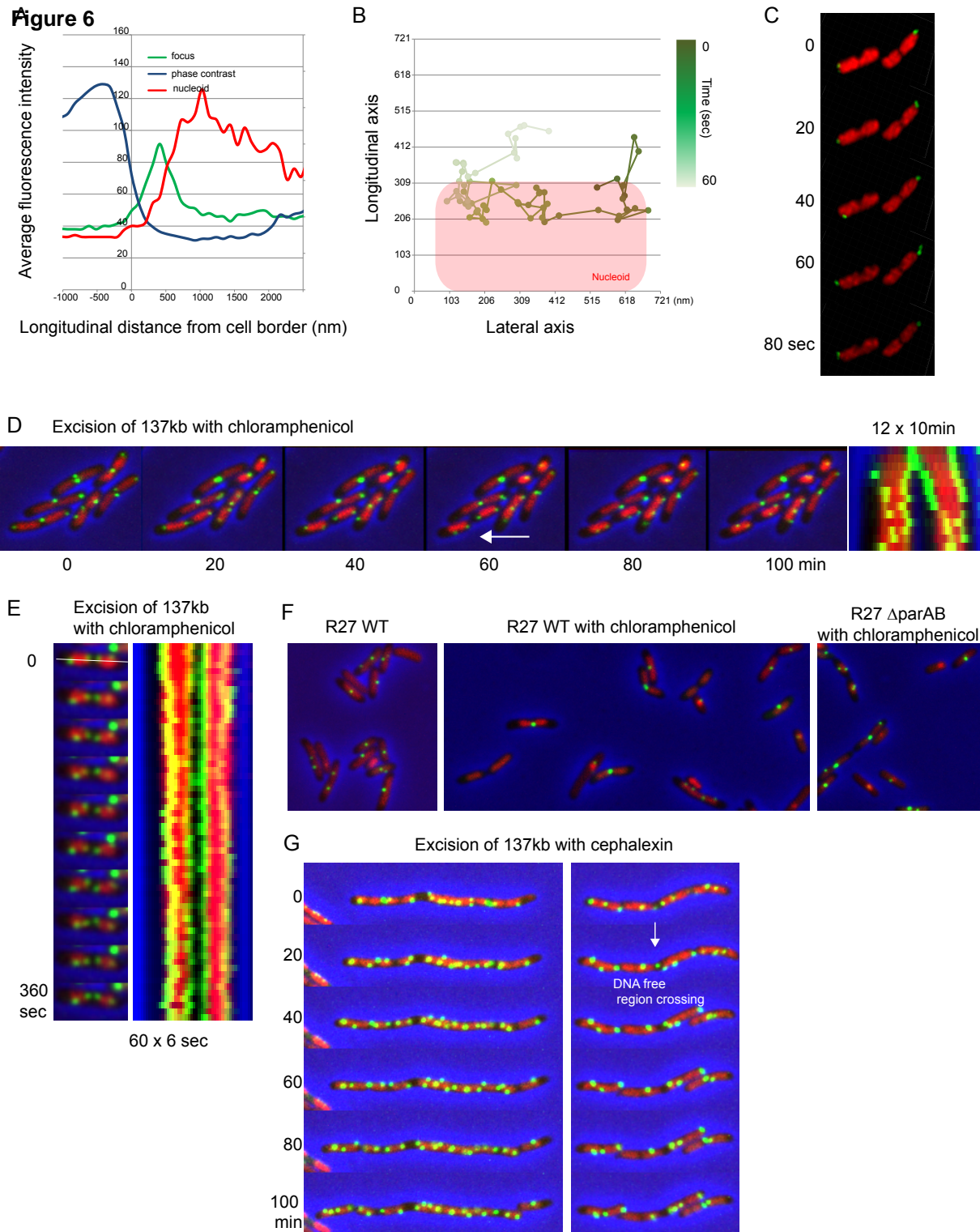


Figure 6

**Supplementary Material figure S1**

[Click here to download Supplementary Material \(To be Published\): fig sup 1.pdf](#)

**Supplementary Material figure S2**

[Click here to download Supplementary Material \(To be Published\): Sup figure free plasmids.pdf](#)

**Supplementary Material figure S3**

[Click here to download Supplementary Material \(To be Published\): Sup figure S2.pdf](#)

**Supplementary Material Table**

[Click here to download Supplementary Material \(To be Published\): Tables\\_S1\\_S2.xlsx](#)